The RXLR-EER Motif Determines an Unconventional Secretion Pathway Associated with Extracellular Vesicle Production

Wei Wang[1]*, Shumei Wang[1*§], Lin Xu[1, 2], Lydia Welsh[3], Petra C Boevink[3], Steve C Whisson[3] & Paul RJ Birch[1,3§].

[1] Division of Plant Sciences, School of Life Science, University of Dundee (at James Hutton Institute), Invergowrie, Dundee DD2 5DA, United Kingdom;

[2] Cell and Developmental Biology Department, John Innes Centre Norwich Research Park, Norwich, United Kingdom;

[3] Department of Cell and Molecular Sciences, James Hutton Institute, Invergowrie, Dundee DD2 5DA, United Kingdom;

* These authors contributed equally to this work

§ Authors for correspondence: P.Birch@dundee.ac.uk; swang002@dundee.ac.uk

Abstract

Phytophthora infestans, the cause of potato late blight disease, delivers a suite of RXLR effectors into host plant cells to subvert immunity, whereas apoplastic effectors act extracellularly. Although the RXLR-EER motif in these effectors is critical for host translocation and is cleaved prior to secretion, the relevance of this processing is poorly understood. Prior evidence suggests RXLR effectors utilize a distinct, unconventional secretion pathway, raising the question of whether the RXLR-EER motif influences selection of the secretion route. Here, we combined genetic, molecular and cell biology approaches to investigate the secretion pathway of RXLR effectors. Confocal microscopy revealed that RXLR and apoplastic effectors localize to distinct vesicular compartments in cultured hyphae. Moreover, fusing the ER retention signal KDEL to RXLR effectors did not impair their secretion, in contrast to apoplastic effectors, which were retained in the endomembrane system, indicating that RXLR effectors bypass the canonical ER-to-Golgi pathway. Importantly, RXLR effectors associate with extracellular vesicles (EVs), whereas RXLR-EER motif mutants show reduced EV association and are rerouted through the ER-to-Golgi secretion pathway. These findings demonstrate that the RXLR-EER motif governs effector sorting into an unconventional, EV-linked secretion route. This study sheds light on the molecular basis of effector trafficking in *P. infestans* and underscores the potential role of EVs in delivering virulence factors during host colonization.

Key words: effector-triggered susceptibility; Golgi-bypass pathway; unconventional secretion

Introduction

The oomycete *Phytophthora infestans* is the causative agent of potato late blight, a devastating disease that triggered the Irish potato famine in the 19th century and continues to pose a major threat to global food security [1, 2]. As a highly adapted hemi-biotrophic pathogen, *P. infestans* relies on a large and complex suite of effector proteins to manipulate host cell physiology and suppress immune responses, enabling successful colonization and disease progression.

The effectors can be broadly divided into two classes based on their site of action: apoplastic effectors, which are secreted into the extracellular space (apoplast) [3], where they act on the outside of plant cells, and cytoplasmic effectors with an Arg-any amino acid-Arg-Leu (RXLR) motif, downstream of a secretion signal peptide, often followed closely by EER (Glu-Glu-Arg) motif, which are encoded by hundreds of genes within the genomes of *Phytophthora* spp. and downy mildew pathogens [4, 5, 6]. RXLR effectors are delivered into the host cell cytosol and target multiple proteins and processes at diverse subcellular locations to suppress immunity [7, 8, 9, 10]. Whereas apoplastic effectors may be perceived by host pattern recognition receptors (PRRs) at the cell surface, RXLR effectors interfere with intracellular immunity by targeting various host processes within plant cells and can, in turn, be perceived by nucleotide-binding leucine-rich repeat receptors [11]. The RXLR-EER motif is crucial for host cell translocation and is proteolytically cleaved prior to secretion, although the functional consequences of this processing are poorly understood [12, 13, 14].

Previous studies show that apoplastic effectors in *P. infestans* are secreted via the conventional ER-to-Golgi pathway, as indicated by their sensitivity to the inhibitor brefeldin A (BFA). In contrast, RXLR effectors are largely BFA-insensitive, suggesting they follow an unconventional secretion route[15, 16]. A similar dichotomy in effector secretion has been observed in the fungal pathogen of rice, *Magnaporthe oryzae*, where cytoplasmic effectors are delivered via a BFA-insensitive, non-classical pathway, whereas apoplastic effectors rely on BFA-sensitive ER-to-Golgi trafficking [17]. However, it is important to recognise that BFA treatment can have off-target or pleiotropic effects, including disruption of endosomal trafficking, vesicle recycling, and broader alterations in membrane dynamics [18]. These side-effects may complicate interpretation of BFA sensitivity assays, particularly in complex filamentous pathogens such as *P. infestans*, where multiple secretory routes may coexist. Therefore, while BFA sensitivity provides a useful initial indication of secretory pathway involvement, additional genetic and imaging-based approaches are essential to unambiguously distinguish between conventional and unconventional secretion routes.

Recently, emerging evidence suggests that RXLR effectors are secreted via an unconventional pathway potentially associated with production of extracellular vesicles (EVs)[19]. EVs are membrane-bound nanoparticles released by cells into the extracellular milieu and have been increasingly recognized as vehicles for intercellular communication and molecular cargo delivery between organisms from different kingdoms[20]. Recently, EVs have been shown to play a pivotal bidirectional transport role in plant–pathogen interactions [21, 22, 23, 24, 25]. In addition to the intriguing link between EVs and effector trafficking, the mechanisms by which RXLR effectors are sorted to EVs, and the signals that determine their route of secretion, are largely unknown. In particular, whether the RXLR-EER motif influences intracellular sorting within the pathogen secretory systems has yet to be resolved.

In this study, we combined molecular, genetic and live-cell imaging approaches to investigate the secretion pathway of RXLR effectors in *P. infestans*. To determine whether these effectors utilize the classical ER–to-Golgi secretion route, we fused a canonical ER retention signal, KDEL (Lys-Asp-Glu-Leu), to RXLR effectors. The KDEL motif, typically found at the C-

terminus of ER-resident proteins, is recognized by KDEL receptors in the cis-Golgi, which mediate the retrograde transport of these proteins back to the ER. While apoplastic effectors were largely retained in the ER after the addition of KDEL, RXLR effectors remained efficiently secreted, suggesting that they bypass the conventional ER–to-Golgi pathway. Furthermore, site-directed mutagenesis of the RXLR-EER motifs redirected these effectors to the classical ER-to-Golgi secretion route and disrupted their association with EVs, indicating that the RXLR-EER motif plays a role in effector trafficking within the pathogen.

Our findings provide compelling evidence that the RXLR-EER motif governs effector trafficking within *P. infestans*, channelling them into an unconventional secretory route linked to EV production. This study deepens our understanding of effector biogenesis and secretion and highlights EVs as potential mediators of virulence protein delivery in plant-pathogen interactions.

Results

RXLR effectors and apoplastic effectors are associated with different types of trafficking vesicles

Previous studies have shown that the secretion of RXLR effectors in *P. infestans* is largely insensitive to BFA, whereas the secretion of apoplastic effectors is BFA-sensitive. This differential response suggests that RXLR and apoplastic effectors utilize distinct secretion pathways [15, 16]. To further explore this hypothesis, we co-expressed two apoplastic effectors, PiSCR74 and PiEPIC1, each C-terminally tagged with fluorescent proteins (mCitrine or mCherry respectively), in *P. infestans* and analyzed their localization using confocal microscopy. The two proteins exhibited substantial co-localization in puncta in cultured hyphae, consistent with the previous observations[15, 16] that they are both trafficked through the conventional ER-to-Golgi secretory pathway (Fig. 1a). We have shown that RXLR effectors Pi04314 and Pi09216 strongly co-localized at vesicle-like structures in cultured hyphae[19]. Consistent with these findings, co-expression of Pi04314 and PiAVRblb1 also revealed robust co-localization at puncta in hyphae, reinforcing the concept that RXLR effectors follow a common intracellular trafficking route (Supplementary Fig. 1). In contrast, when apoplastic effector PiSCR74 was co-expressed with RXLR effector Pi04314, the two proteins localized to distinct vesicle-like compartments, providing supporting evidence that RXLR and apoplastic effectors are sorted through different secretory routes (Fig. 1b).

To investigate whether these effectors are associated with distinct populations of endosomal vesicles, we isolated endo-vesicles from cultured mycelia using a sucrose gradient that was bottom-loaded to allow vesicles to rise to their buoyant density and thus exclude protein aggregates (Supplementary Fig. 2a). Transmission electron microscopy of the vesicle fractions (VFs) confirmed the presence of typical membrane-bound vesicles (Supplementary Fig. 2b). Confocal imaging of the VFs revealed that fluorescent protein tagged PiSCR74 and PiEPIC1 largely co-localized within the same vesicle population. Furthermore, fluorescence signals from both effector fusions were abolished by pre-treatment with 1% TritonX-100 detergent, which disrupts lipid membranes but not protein aggregates[26, 27] (Fig. 1c). Similarly, two fluorescently tagged RXLR effectors Pi04314 and PiAVRblb1 largely co-localized within the same vesicle population (Supplementary Fig. 2c). In contrast, Pi04314 and PiSCR74 fusions localized to separate vesicle populations. Similarly, their respective fluorescence signals were also detergent-sensitive, indicating membrane association (Fig. 1d). Immunoblot analysis confirmed that apoplastic and RXLR effectors were all present as intact fusion proteins in the vesicle fractions, and that detergent treatment abolished their presence in VFs (Supplementary

Fig. 2d). These results indicate their association with membrane-bound vesicular structures, supporting the conclusion that RXLR and apoplastic effectors are sorted into distinct vesicle types and follow different secretion pathways in *P. infestans*.

RXLR effectors follow a Golgi-independent route after cleavage

Given that apoplastic effectors are secreted via the conventional ER-to-Golgi pathway and that RXLR effectors are insensitive to BFA treatment, we hypothesized that RXLR effectors utilize a Golgi-bypass secretion mechanism. To test this hypothesis, we employed a molecular strategy involving the addition of an ER retention signal—KDEL (Lys-Asp-Glu-Leu)—to the C-terminus of effector-fluorescent protein fusions. The KDEL motif is recognized by KDEL receptors (KDELRs) located in the cis-Golgi, which mediate retrograde transport of KDEL-tagged proteins back to the ER [28]. Proteins secreted via a Golgi-independent route would be expected to escape this retention mechanism. To evaluate this, apoplastic (PiSCR74 and PiEPIC1) or RXLR (Pi04314 and PiAVRblb1) effector fluorescence protein fusions either with or without the KDEL motif, were expressed in *P. infestans* strains cultured in liquid medium. Immunoblotting revealed that apoplastic effectors were efficiently secreted under normal conditions, but their secretion was markedly reduced upon addition of KDEL, whereas the secretion of RXLR effectors was largely unaffected, indicating that their export does not primarily depend on Golgi-mediated trafficking (Fig. 2a).

We validated these findings *in planta* using confocal microscopy. All effectors accumulated at the haustorial interface under normal conditions. However, upon KDEL addition, apoplastic effectors accumulated in ER-like endomembrane compartments, consistent with receptor-mediated retention. In contrast, RXLR effectors accumulated at the haustorial interface even when fused to KDEL (Fig. 2b). These results strongly support the conclusion that apoplastic effectors are secreted through a conventional ER-Golgi pathway, whereas RXLR effectors are exported via a Golgi-bypass mechanism.

Our previous work showed that the RXLR-EER motif is not recognized or correctly cleaved in plant cells[14]. To determine whether proteolytic processing of this motif influences the pathway of secretion, the RXLR effector Pi04314 — with or without its native signal peptide (SP) — was transiently expressed in *Nicotiana benthamiana*. Confocal microscopy revealed that the SP-containing version was secreted into the apoplast, whereas the version lacking the SP localized to the nucleus or nucleolus, the expected site of the effector activity *in planta* [29, 30]. While BFA treatment disrupted secretion of SP-tagged Pi04314, causing it to accumulation in BFA bodies[31], it did not alter the subcellular localization of NSP-Pi04314 (Supplementary Fig. 3a). Addition of a C-terminal KDEL motif caused SP-04314-RFP to be retained in the ER (Supplementary Fig. 3b), confirming that uncleaved RXLR effectors follow the conventional ER-to-Golgi pathway in plant cells. These results highlight the importance of appropriate perception and cleavage of the RXLR-EER motif in directing these effectors toward an alternative, Golgi-bypass secretion route.

The RXLR-EER motif determines the secretion pathway.

Given that the RXLR-EER motif functions as a protease processing site prior to secretion [13, 14], we sought to investigate whether this motif also determines the secretion route of RXLR effectors. In previous work, we showed that RXLR-EER motif mutants could still be secreted at haustoria[14], but it is unclear if the secretion pathway was altered. To test this, we generated a mutant version of the RXLR effector Pi04314 in which the RXLR-EER motif was substituted with alanines (Pi04314-7A). Both wild-type (WT) and mutant versions were fused with different fluorescent proteins (mCherry or mCitrine) and co-expressed in *P. infestans*. Confocal microscopy of cultured hyphae revealed that the WT and mutant effectors localized to distinct

vesicular compartments (Fig. 3a). Notably, the Pi04314-7A mutant co-localized significantly with apoplastic effector PiSCR74 (Fig. 3b), suggesting a shift in its trafficking route. Endo-vesicle isolation from the same transformants confirmed that the RXLR-EER mutant was sorted into vesicles distinct from those carrying the wild-type RXLR effectors (Fig. 3c), but largely co-localized with vesicles associated with apoplastic effector PiSCR74 (Fig. 3d). Importantly, addition of a KDEL motif to the RXLR-EER 7A mutants, for both Pi04314 and PiAVRblb1, significantly impaired their secretion into the culture medium (culture filtrate, CF) (Fig. 3e, Supplementary Fig. 4a). *In planta*, these KDEL-tagged mutants displayed ER retention patterns similar to those observed for KDEL-tagged apoplastic effectors (Fig. 3f, Supplementary Fig. 4b). These findings indicate that the RXLR-EER motif plays a key role in directing RXLR effectors into an unconventional, Golgi-independent secretion pathway, and its mutation leads to conventional ER-to-Golgi secretion.

The RXLR-EER motif governs the association of RXLR effectors with EVs

Our recent work suggested that RXLR effectors such as Pi04314 and PiAVRblb1 are associated with pellets containing EVs[19]. Pi04314 was also shown to co-localize, prior to secretion, with two candidate EV markers, PiMDP1 and PiMDP2 in hyphal endo-vesicles[19]. To investigate whether the RXLR-EER motif governs this co-association, we examined WT and RXLR-EER mutant versions of the effectors (Pi04314-7A and PiAVRblb1-7A) using EVs isolated from cultured mycelia and western blotting. Although the mutants were still detected in pellets containing EVs, their abundance that relative to total secretion (CF) was significantly reduced compared to the WT proteins, indicating diminished association with EVs (Fig. 4a). In contrast, the addition of a C-terminal KDEL motif to the WT Pi04314 or PiAVRblb1did not affect EV association (Fig. 4a), consistent with our findings that KDEL does not alter the secretion route of RXLR effectors (Fig. 2a, b).

To further assess the role of the RXLR-EER motif in EV targeting, Pi04314-7A was co-expressed with the EV marker PiMDP1 in *P. infestans*. Confocal microscopy showed no co-localization between the mutant and PiMDP1 in cultured hyphae, and they were found in distinct endo-vesicle populations (Fig. 4b, c; Supplementary Fig. 5a). In contrast, WT Pi04314 strongly co-localized with PiMDP1 in the same endo-vesicle types (Supplementary Fig. 4b, c). Together, these findings demonstrate that the RXLR-EER motif and its processing are key determinants of RXLR effector sorting into an unconventional secretion pathway associated with EV production.

Discussion

Our study provides compelling cell biological and genetic evidence that *P. infestans* deploys distinct secretion pathways for two major classes of effector proteins—apoplastic and RXLR-type cytoplasmic effectors. Whereas apoplastic effectors are secreted via the conventional ER-to-Golgi pathway, RXLR effectors utilize an unconventional secretion route that bypasses the Golgi. Critically, we demonstrate that the RXLR-EER motif is essential for determining the unconventional secretion of these cytoplasmic effectors and their association with extracellular vesicles (EVs) (Supplementary Fig 6).

Previously, sensitivity to the inhibitor BFA was used to distinguish between *P. infestans* apoplastic and cytoplasmic (RXLR) effector secretion pathways [15, 16]. This approach was used also to demonstrate that apoplastic and cytoplasmic effectors from the fungal pathogen of rice and wheat, *Magnaporthe oryzae*, were also secreted by conventional and unconventional pathways, respectively [17]. However, BFA treatment can have off-target effects [18]. As such, non-disruptive cell biological and genetic approaches are required to confirm inhibitor-based

228 studies. We found that apoplastic effectors and RXLR effectors did not co-localise at mobile
229 endo-vesicles in *P. infestans* hyphae (Fig 1), consistent with their secretion via different
230 pathways. Critically, whereas addition of a KDEL motif to the C-terminus of apoplastic
231 effectors resulted in their retention in hyphae, consistent with retrograde trafficking of them
232 from the Golgi to the ER, addition of a KDEL motif to RXLR effectors did not prevent their
233 secretion (Fig 2; Supplementary Fig 6). These cell biological and genetic approaches, which
234 agree with previously published BFA results [15,16], offer a non-disruptive means to distinguish
235 between conventional and unconventional secretion pathways that could be adopted to verify
236 previous findings in other fungi such as *M. oryzae* [17] and investigate effector secretion in other
237 pests and pathogens of plants or animals.

238 Importantly, we identified the RXLR-EER motif as a key determinant of unconventional
239 secretion of these effectors. Mutating the RXLR-EER motif not only altered the intracellular
240 localization of RXLR effectors—leading them to co-localize in endo-vesicles with apoplastic
241 effectors—but also shifted their secretion to a Golgi-dependent route (Fig. 3). When the RXLR-
242 EER motif was mutated, effectors were retained in the ER upon addition of a KDEL tag,
243 confirming they were secreted conventionally via the Golgi (Supplementary Fig. 3). We thus
244 argue that the RXLR-EER motif acts as an ER sorting signal to an unconventional, Golgi-
245 bypass secretion pathway. Importantly, secretion of the WT RXLR effector Pi04314-mRFP by
246 the plant *N. benthamiana* followed a conventional ER-to-Golgi pathway that was BFA-
247 sensitive and prevented by addition of a KDEL motif (Supplementary Fig. 3). As we showed
248 previously that there is no efficient proteolytic cleavage of Pi04314 during secretion by *N.*
249 *benthamiana*[14] this strongly implicates such processing of the RXLR-EER motif as a
250 requirement for sorting into an unconventional secretion pathway. Interestingly, our recent
251 observation that RXLR effectors are often associated with extracellular vesicles (EVs),
252 whereas apoplastic effectors are not[19], provides further evidence that these effector classes
253 follow distinct secretion pathways. Our data here demonstrate that the RXLR-EER motif also
254 governs the association of RXLR effectors with EVs. Whereas WT RXLR effectors co-
255 localized with EV markers and were enriched in EV pellets, their RXLR-EER mutants showed
256 diminished EV-association and failed to co-localize with EV markers (Fig. 4, Supplementary
257 Fig. 5). This suggests that the RXLR-EER motif has a critical role in the intracellular sorting
258 of RXLR effectors toward an unconventional pathway associated with EV production
259 (Supplementary Fig 6).

260 The *Phytophthora* RXLR effectors have been described as analogous to PEXEL effectors
261 delivered into human cells by the distantly-related apicomplexan malaria pathogen
262 *Plasmodium falciparum* [32]. PEXEL effectors contain a related motif, RxLxE/D/Q, which is also
263 proteolytically processed during secretion [33]. The precise role of this motif remains unclear.
264 Our findings reveal a role for the RXLR-EER motif in directing RXLR effectors to an
265 unconventional secretion pathway that bypasses the Golgi following proteolytic cleavage. This
266 is different to PEXEL effectors from *Plasmodium* which, following proteolytic cleavage in the
267 ER, are secreted through the ER-to-Golgi pathway [34]. Future studies should focus on
268 identifying the molecular machinery that processes RXLR-EER motifs within *Phytophthora*
269 and mediates their sorting into an unconventional secretion pathway associated with EV
270 production. This machinery could represent a novel target for disease control.

271

272 **Methods**

273 ***Phytophthora infestans* growth and plant growth**

Phytophthora infestans (*P. infestans*) strain 3928A, along with its derived transgenic lines, was cultured on Rye Agar medium supplemented with Ampicillin (100 µg/ml) and Pimaricin (0.02%). Geneticin (10 µg/ml) was included to ensure the selection and maintenance of transgenic lines. *Nicotiana benthamiana* and the susceptible potato cultivar Solanum tuberosum 'Maris Piper' were grown in controlled glasshouse conditions under a 16-hour light/8-hour dark cycle.

To assess the secretion efficiency of *P. infestans*. A 14-day old plate was flooded with 3ml amended lima bean (ALB) liquid media supplemented with the appropriate antibiotics scraped with a sterile spreader and grown for 1 days in the dark without shaking. Mycelia were transferred into fresh culture tubes containing 1.5 ml ALB (with appropriate antibiotics) which had been pre-cleared by ultracentrifugation at 120 000 × g for 2 hours. Cultures were grown for a further day.

For EV/Endo-vesicle isolation. At least two 14-day old plates were flooded with 15ml amended lima bean (ALB) liquid media supplemented with the appropriate antibiotics. Sporangia were collected by pouring the suspension into a sterile culture bottle through a 70 µm cell strainer. Sporangia were allowed to grow for 2 days (or 4 days for endo-vesicle isolation) in the dark without shaking. To isolate EVs, mycelia were transferred into fresh culture bottles containing 15 ml minimal media and 15 ml ALB which had been pre-cleared by ultracentrifugation at 120, 000*g* for 2 h. Cultures were grown for a further 2 days.

Construction of *P. infestans* transgenic lines

The vector pmCitrine:mCherry, designed for co-expression of proteins tagged with mCitrine and mCherry, was constructed by Breen et al., (2025)[19]. The coding sequence for PiSCR74 was amplified from a published vector[35]. Coding sequences for PiEPIC1 (PITG_09169) and Pi04314 (PITG_04314) were amplified from published vectors constructed by Wang et al., (2017, 2018)[15, 16], and PiAVRblb1 (PITG_21388) and all RXLR-EER mutated versions were amplified from published vector generated by Xu et al., (2025)[14], using primers listed in Supplementary Table 1. KDEL motif was synthesised with restriction enzyme sites (Supplementary Table 1). These coding sequences were cloned as C-terminal fusions to the fluorescent proteins, driven by the oomycete Ham34 promotor (Ham34P)[36], using restriction enzyme cloning and standard molecular biology techniques. Plasmids were sequenced to verify the correct insertion of target sequences and prepared for downstream applications using the Promega PureYield™ Plasmid Maxiprep System. Transformation of *P. infestans* isolate 3928A was conducted following the protocol described by Welsh et al. (2025)[37].

Construction of expression vectors and transient expression *in planta*

The *P. infestans* genes encoding Pi04314, PiSCR74, or PiAVRblb1, including their native predicted signal peptides and C-terminally fused mCherry, with or without a KDEL motif, were amplified from above constructed vectors used in *P. infestans* transformations. The vector lacking the signal peptide (NSP-Pi04314-mRFP) was generated by Wang et al. (2017)[15], while the NSP-PiAVRblb1-mRFP construct was produced by Xu et al. (2025)[14]. Gene-specific primers containing flanking Gateway recombination sites were used for PCR amplification (Supplementary Table 1). The purified PCR products were recombined into the entry vector pDONR201 (Invitrogen) to generate entry clones. These entry clones were subsequently recombined with the binary vector pK7WG2 and transformed into *Agrobacterium tumefaciens* strain GV3101 for transient expression in *Nicotiana benthamiana*[38]. *A. tumefaciens* cultures were infiltrated at an OD_{600} of 0.05. Brefeldin A (BFA) was applied at a final concentration of 20 µg/mL, 30–60 minutes prior to imaging, as previously described Wang et al., (2017)[15].

Immunoblotting and quantification

321 For protein extraction from *P. infestans* mycelia, approximately 0.01 g of fresh mycelium was
322 collected in a 1.5 ml Eppendorf tube and mixed with 80 µl of 2× SDS buffer (to assess the
323 overall secretion efficiency, all obtained mycelia were collected in a 1.5 ml Eppendorf tube and
324 ground with a pestle in 150 µl of 2× SDS buffer.). The sample was vortexed for 1 minute and
325 subsequently boiled at 95°C for 10 minutes. For protein extraction from culture filtrate and
326 supernatant, total proteins were isolated using the chloroform/methanol precipitation method[39].
327 Briefly, 4 ml of methanol, 1 ml of chloroform, and 4 ml of sterile water were added to 1 ml of
328 liquid samples. To assess the overall secretion efficiency, all resulted culture filtrate (~1.5 ml)
329 was used for precipitation. The mixture was thoroughly vortexed and centrifuged at 5000 × g
330 for 20 minutes. The precipitated proteins were washed with 3 ml of absolute methanol, and the
331 air-dried pellet was resuspended in 80 µl of 2× SDS loading buffer.

332 Samples were loaded onto 10% SDS-PAGE gels and transferred onto nitrocellulose
333 membranes. Membranes were blocked for one hour at room temperature in 4% milk dissolved
334 in 1× PBST (0.05% Tween 20). Primary antibodies targeting RFP/mCherry (Chromotek, 58F)
335 and GFP/mCitrine (Roche, 11814460001) were diluted to 1:4000 and 1:2000, respectively, in
336 blocking buffer and incubated with the membranes overnight at 4°C or room temperature for 2
337 hours. Following incubation, membranes were washed five times (10 minutes for each time)
338 with 1× PBST. Secondary antibodies—IRDye® 680RD Goat anti-Rat IgG, IRDye® 800CW
339 Goat anti-Mouse IgG (LI-COR Biosciences)—were added at a 1:5000 dilution in blocking
340 buffer. Membranes were incubated with secondary antibodies for one hour at room temperature
341 in the dark. Signal detection and quantification were performed using the LI-COR
342 ODYSSEY® DLx imaging system and LICOR Image Studio™ software.

343 **Endo-vesicles isolation from *P. infestans***

344 Endo-vesicles from *P. infestans* were isolated using 1–2 g of mycelia homogenized in an equal
345 volume of isolation buffer (150 mM Na-HEPES, pH 7.5, 10 mM EDTA, 10 mM EGTA, 17.5%
346 [w/w] sucrose, 7.5 mM KCl, 10 mM DTT, 1× PIC-W, 1× PIC-D, and 1× E-64) as described by
347 Wang et al. (2023)[40]. For samples designated for Triton X-100 treatment, the supernatant was
348 divided into two equal volumes. One portion was treated with Triton X-100 to a final
349 concentration of 1%, while the other received an equivalent volume of sterile distilled water as
350 a control. All samples were thoroughly mixed and incubated on ice for one hour. After
351 incubation, the samples were adjusted to 40.6% (w/w) sucrose by mixing with 62% (w/w)
352 sucrose solution. A 2.4 mL aliquot of this sucrose mixture was loaded at the bottom of a 13.2
353 mL ultracentrifuge tube and overlaid sequentially with 3 mL of 35% (w/w) sucrose, 3 mL of
354 25% (w/w) sucrose, and 3 mL of 8.5% (w/w) sucrose to form a gradient. The loaded gradient
355 was centrifuged at 400,000*g* for 3 hours at 4 °C using a Beckman Coulter SW 41 Ti rotor. The
356 two interfaces between the 8.5% and 25%, 25% and 35% sucrose layers was carefully collected
357 and pelleted by ultracentrifugation at 100,000*g* for 1 hour at 4 °C. Pellets were prepared for
358 microscopy analysis and immunoblotting. All sucrose solutions were prepared in 150 mM Na-
359 HEPES buffer (pH 7.5) and included protease inhibitors (1× PIC-W, 1× PIC-D, and 1× E-64)
360 to ensure vesicle integrity.

361 **Transmission microscopy (TEM)**

362 25 µl of endo-vesicle samples or buffer control was mixed with 25 µl of 4% paraformaldehyde
363 (PFA) in 0.1 M sodium phosphate pH 7.4 to give a final concentration of 2% PFA. 30 µl aliquots
364 were pipetted onto Parafilm with nickel grids (carbon-coated, formvar, 300 mesh) placed on
365 top, and incubated at room temperature for 30 minutes. Grids were washed with 1x PBS twice
366 and incubated for 10 minutes with 50µl 1% glutaraldehyde. Grids were then washed with 100
367 µl sterile water seven times and stained with 4% uranyl oxalate for 10 minutes at room
368 temperature. Grids were transferred onto two 50 µl drops of uranyl acetate (0.15%

methylcellulose and 0.4% uranyl acetate) sequentially and left on the second drop for 10 minutes on ice. Excess liquid was wicked off with filter paper and grids were inspected with a JEOL 1400 at 80 kV.

Confocal microscopy and data quantification

P. infestans hyphae grown in ultracentrifugation cleaned ALB medium on microscope slides were imaged at 1–2 days post-inoculation, while leaf infections on *Solanum tuberosum* were imaged at 2–3 days post-inoculation. *N. benthamiana* leaves were imaged at 2 days after *Agrobacterium* infiltration. Imaging was performed using a Nikon A1R confocal microscope.

For GFP fluorescence, the 488 nm line from an argon laser was used for excitation, and emissions were collected between 500–530 nm. For mCitrine fluorescence, the 514 nm line from an argon laser was used for excitation, and emissions were collected between 520–550 nm. For mCherry fluorescence, a 561 nm laser was used for excitation, with emissions collected between 600–630 nm. The pinhole was set to 1.2 airy unit to optimize resolution. Images were processed using OMERO, or ImageJ software. To assess the effector secretion efficiency during infection, haustoria and adjacent area of invasive hyphae were chosen from single optical sections for measurement. The Fiji plugin DiAna was used for endo-vesicle co-localization analyses[41].

EV isolation from *P. infestans* culture

EVs were isolated from *P. infestans* culture as described before[19]. Approximately 30 ml culture was used for EV isolation. 1 ml of culture filtrate (CF) was collected after the removal of mycelia using a 70 µm cell strainer. The filtered CF was centrifuged for 10 minutes at 2000*g* and filtered through a 0.45 µm syringe filter, following a further spin at 10,000*g* for 30 minutes to remove all cellular debris and large vesicles. Supernatant from previous step was then ultracentrifuged at 100,000*g* for 1 hour at 4 °C (Beckman Coulter Type50.2 Ti rotor) to finally obtain the crude EV pellet (P) samples, pellet was dissolved in 80 µl SDS buffer for western blot.

Acknowledgements

We are grateful to colleagues Drs Hazel McLellan and Susan Breen for helpful discussions during the development of this research. We thank Dr Kasia Mackinnon for technical support. The research was supported by United Kingdom Research and Innovation Horizon Europe Guarantee Marie Skłodowska-Curie Actions Postdoctoral Fellowship (EP/Z00196X/1); Biotechnology and Biological Sciences Research Council grants BB/Z515115/1 and BB/Z517495/1; European Research Council (ERC)-Advanced grant PathEVome (787764); and Scottish Government Rural and Environment Science and Analytical Services Division (RESAS) JHI B1-1.

Author contributions

S.W., W.W and P.R.J.B. conceived of and designed the research; S.W. and W.W. performed the research; L.X provided resources of *P. infestans* transformants; L.W. provided technical support; S.W., W.W and P.R.J.B. analysed data; S.W., P.R.J.B., S.C.W. and P.C.B. won funding for the research; and S.W., W.W and P.R.J.B. wrote the paper with input from all co-authors.

The authors declare no competing interest.

413 **References**

414 1. Fry WE, *et al.* Five Reasons to Consider Phytophthora infestans a Reemerging
415 Pathogen. *Phytopathology* **105,** 966-981 (2015).
416 2. Kamoun S, *et al.* The Top 10 oomycete pathogens in molecular plant pathology. *Mol*
417 *Plant Pathol* **16,** 413-434 (2015).
418 3. Tanaka S, Kahmann R. Cell wall-associated effectors of plant-colonizing fungi.
419 *Mycologia* **113,** 247-260 (2021).
420 4. Kronmiller BA, *et al.* Comparative Genomic Analysis of 31 Phytophthora Genomes
421 Reveals Genome Plasticity and Horizontal Gene Transfer. *Mol Plant Microbe In* **36,**
422 26-46 (2023).
423 5. Mandal K, Dutta S, Upadhyay A, Panda A, Tripathy S. Comparative Genome
424 Analysis Across 128 Isolates Reveal Species-Specific Microsatellite Distribution and
425 Localized Evolution of Compartmentalized Genomes. *Frontiers in Microbiology* **13,**
426 (2022).
427 6. Tör M, Wood T, Webb A, Göl D, McDowell JM. Recent developments in plant-downy
428 mildew interactions. *Seminars in Cell & Developmental Biology* **148,** 42-50 (2023).
429 7. He Q, McLellan H, Boevink PC, Birch PRJ. All Roads Lead to Susceptibility: The
430 Many Modes of Action of Fungal and Oomycete Intracellular Effectors. *Plant*
431 *Commun* **1,** 100050 (2020).
432 8. Petre B, *et al.* Host-interactor screens of Phytophthora infestans RXLR proteins reveal
433 vesicle trafficking as a major effector-targeted process. *Plant Cell* **33,** 1447-1471
434 (2021).
435 9. McLellan H, *et al.* Exploiting breakdown in nonhost effector-target interactions to
436 boost host disease resistance. *Proc Natl Acad Sci U S A* **119,** e2114064119 (2022).
437 10. Wang S, McLellan H, Boevink PC, Birch PRJ. RxLR Effectors: Master Modulators,
438 Modifiers and Manipulators. *Mol Plant Microbe Interact* **36,** 754-763 (2023).
439 11. Sundaram B, Tweedell RE, Kumar SP, Kanneganti TD. The NLR family of innate
440 immune and cell death sensors. *Immunity* **57,** 674-699 (2024).
441 12. Whisson SC, *et al.* A translocation signal for delivery of oomycete effector proteins
442 into host plant cells. *Nature* **450,** 115-+ (2007).
443 13. Wawra S, *et al.* The RxLR Motif of the Host Targeting Effector AVR3a of
444 Phytophthora infestans Is Cleaved before Secretion. *Plant Cell* **29,** 1184-1195 (2017).
445 14. Xu L, *et al.* Proteolytic processing of both RXLR and EER motifs in oomycete
446 effectors. *New Phytologist* **245,** 1640-1654 (2025).
447 15. Wang S, Boevink PC, Welsh L, Zhang R, Whisson SC, Birch PRJ. Delivery of
448 cytoplasmic and apoplastic effectors from Phytophthora infestans haustoria by distinct
449 secretion pathways. *New Phytol* **216,** 205-215 (2017).
450 16. Wang S, Welsh L, Thorpe P, Whisson SC, Boevink PC, Birch PRJ. The Phytophthora
451 infestans Haustorium Is a Site for Secretion of Diverse Classes of Infection-
452 Associated Proteins. *mBio* **9,** (2018).
453 17. Giraldo MC, *et al.* Two distinct secretion systems facilitate tissue invasion by the rice
454 blast fungus Magnaporthe oryzae. *Nat Commun* **4,** 1996 (2013).

18. Lippincott-Schwartz J, Yuan L, Tipper C, Amherdt M, Orci L, Klausner RD. Brefeldin A's effects on endosomes, lysosomes, and the TGN suggest a general mechanism for regulating organelle structure and membrane traffic. *Cell* **67,** 601-616 (1991).
19. Breen S, *et al.* Identification of MARVELous protein markers for Phytophthora infestans extracellular vesicles. Preprint at https://www.biorxiv.org/content/10.1101/2025.04.11.648357v2 (2025).
20. Cai Q, *et al.* Message in a Bubble: Shuttling Small RNAs and Proteins Between Cells and Interacting Organisms Using Extracellular Vesicles. *Annu Rev Plant Biol* **72,** 497-524 (2021).
21. He B, *et al.* Fungal small RNAs ride in extracellular vesicles to enter plant cells through clathrin-mediated endocytosis. *Nat Commun* **14,** 4383 (2023).
22. He B, *et al.* RNA-binding proteins contribute to small RNA loading in plant extracellular vesicles. *Nat Plants* **7,** 342-352 (2021).
23. Wang S, *et al.* Plant mRNAs move into a fungal pathogen via extracellular vesicles to reduce infection. *Cell Host Microbe* **32,** 93-105 e106 (2024).
24. Huang YF, *et al.* Rice extracellular vesicles send defense proteins into fungus to reduce disease. *Dev Cell* **60,** (2025).
25. Koch BL, Rutter BD, Borniego ML, Singla-Rastogi M, Gardner DM, Innes RW. Arabidopsis Produces Distinct Subpopulations of Extracellular Vesicles That Respond Differentially to Biotic Stress, Altering Growth and Infectivity of a Fungal Pathogen. *Journal of Extracellular Vesicles* **14,** (2025).
26. Reid G, *et al.* The human multidrug resistance protein MRP4 functions as a prostaglandin efflux transporter and is inhibited by nonsteroidal antiinflammatory drugs. *P Natl Acad Sci USA* **100,** 9244-9249 (2003).
27. Osteikoetxea X, *et al.* Differential detergent sensitivity of extracellular vesicle subpopulations. Org Biomol Chem **13,** 9775-9782 (2015).
28. Cela I, *et al.* KDEL Receptors: Pathophysiological Functions, Therapeutic Options, and Biotechnological Opportunities. *Biomedicines* **10,** (2022).
29. Boevink PC, *et al.* A Phytophthora infestans RXLR effector targets plant PP1c isoforms that promote late blight disease. *Nat Commun* **7,** 10311 (2016).
30. Bentham AR, Wang W, Trusch F, Varden FA, Birch PRJ, Banfield MJ. The WY Domain of an RxLr Effector Drives Interactions with a Host Target Phosphatase to Mimic Host Regulatory Proteins and Promote Infection. *Mol Plant Microbe In* **37,** 239-249 (2024).
31. Orci L, Perrelet A, Ravazzola M, Wieland FT, Schekman R, Rothman JE. Bfa Bodies - a Subcompartment of the Endoplasmic-Reticulum. *P Natl Acad Sci USA* **90,** 11089-11093 (1993).
32. Horrocks P, Muhia D. PEXEL/VTS: a protein-export motif in erythrocytes infected with malaria parasites. *Trends in Parasitology* **21,** 396-399 (2005).
33. Boddey JA, *et al.* Export of malaria proteins requires co-translational processing of the PEXEL motif independent of phosphoinositol-3-phosphate binding. *Nature Comms* **7,** 10470 (2016)

34. Egea PF. Crossing the vacuolar rubicon: structural insights into effector protein trafficking in apicomplexan parasites. *Microorganisms* **8,** 865 (2020).
35. Lin X, *et al.* Divergent Evolution of PcF/SCR74 Effectors in Oomycetes Is Associated with Distinct Recognition Patterns in Solanaceous Plants. *mBio* **11,** (2020).
36. Judelson HS, Tyler BM, Michelmore RW. Transformation of the Oomycete Pathogen, Phytophthora-Infestans. *Mol Plant Microbe In* **4,** 602-607 (1991).
37. Welsh LRJ, Whisson SC. Protoplast Transformation of Phytophthora spp. *Methods Mol Biol* **2892,** 35-47 (2025).
38. Karimi M, Depicker A, Hilson P. Recombinational cloning with plant gateway vectors. *Plant Physiol* **145,** 1144-1154 (2007).
39. Fic E, Kedracka-Krok S, Jankowska U, Pirog A, Dziedzicka-Wasylewska M. Comparison of protein precipitation methods for various rat brain structures prior to proteomic analysis. *Electrophoresis* **31,** 3573-3579 (2010).
40. Wang H, *et al.* Uptake of oomycete RXLR effectors into host cells by clathrin-mediated endocytosis. *Plant Cell* **35,** 2504-2526 (2023).
41. Gilles JF, Dos Santos M, Boudier T, Bolte S, Heck N. DiAna, an ImageJ tool for object-based 3D co-localization and distance analysis. *Methods* **115,** 55-64 (2017).

515 **Figures**

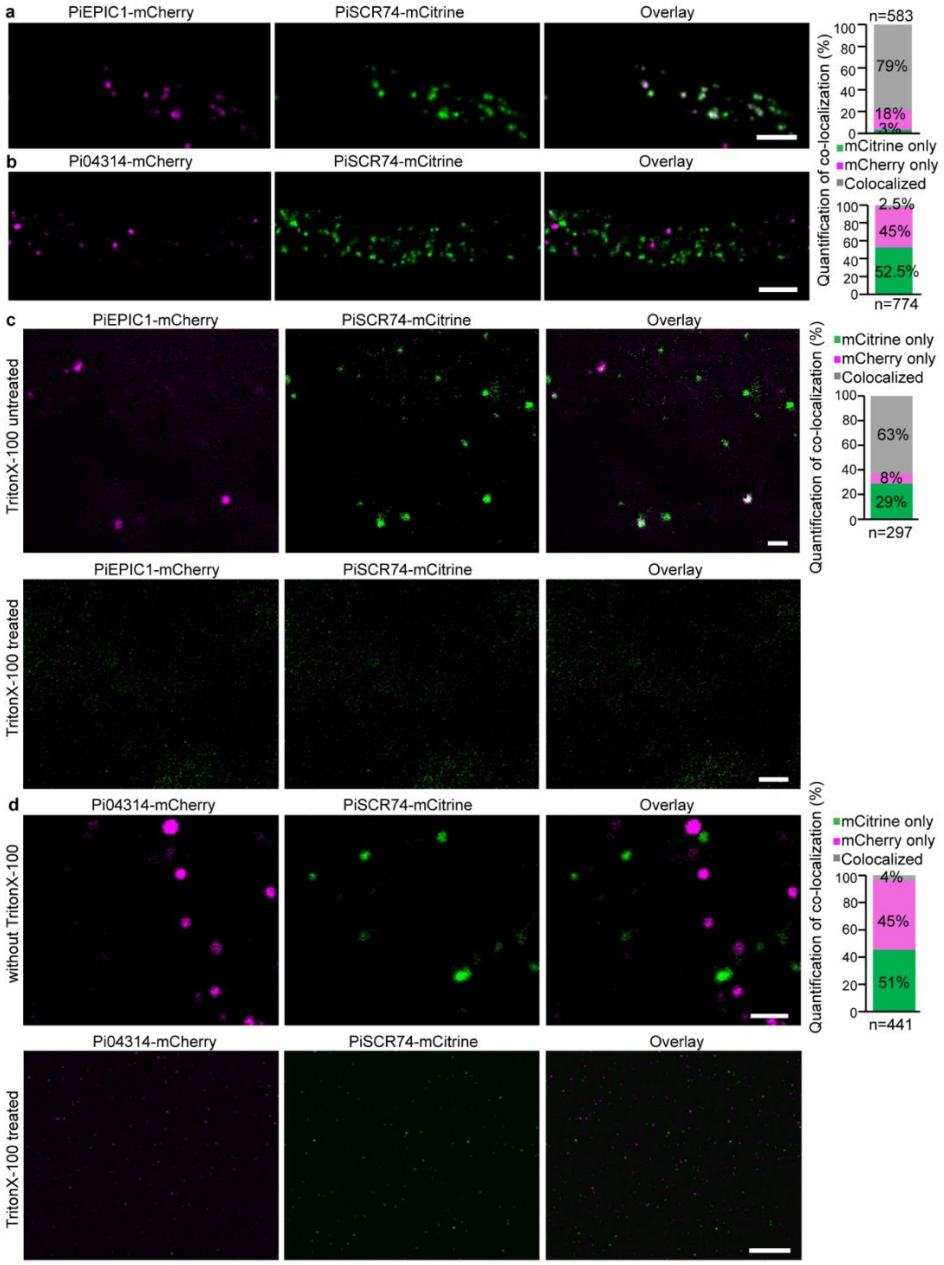

516

517 **Fig. 1| RXLR effectors and apoplastic effectors are associated with different types of**
518 **secretory vesicles. a**, Confocal microscopy images showing colocalization of PiSCR74-
519 mCitrine with PiEPIC1-mCherry in puncta in cultured hyphae. **b**. PiSCR74-mCitrine co-
520 expressed with the RXLR effector Pi04314-mCherry, showing a lack of colocalization in
521 puncta in cultured hyphae. Scale bars, 10 µm (**a**, **b**). **c**, Endosomal vesicles isolated from the
522 same dual transformants shown in **a** confirm colocalization between the apoplastic effectors
523 (upper panel). Treatment with 1% Triton X-100 disrupts vesicle integrity, indicating that the
524 punctate structures are membrane-bound (lower panel). Quantification of colocalization is
525 shown in the accompanying graphs. **d,** Endosomal vesicles isolated from the same dual
526 transformants as in **b** show almost no colocalization between Pi04314 and PiSCR74. Treatment
527 with 1% Triton X-100 confirms both effectors are associated with membrane structures. Scale
528 bars, 2 µm (**c**–**d**). Quantification of colocalization is presented in the accompanying graphs.
529 The numbers of total and co-labelled puncta were determined using the DiAna plugin in Fiji
530 (**a**–**d**). n=total puncta.

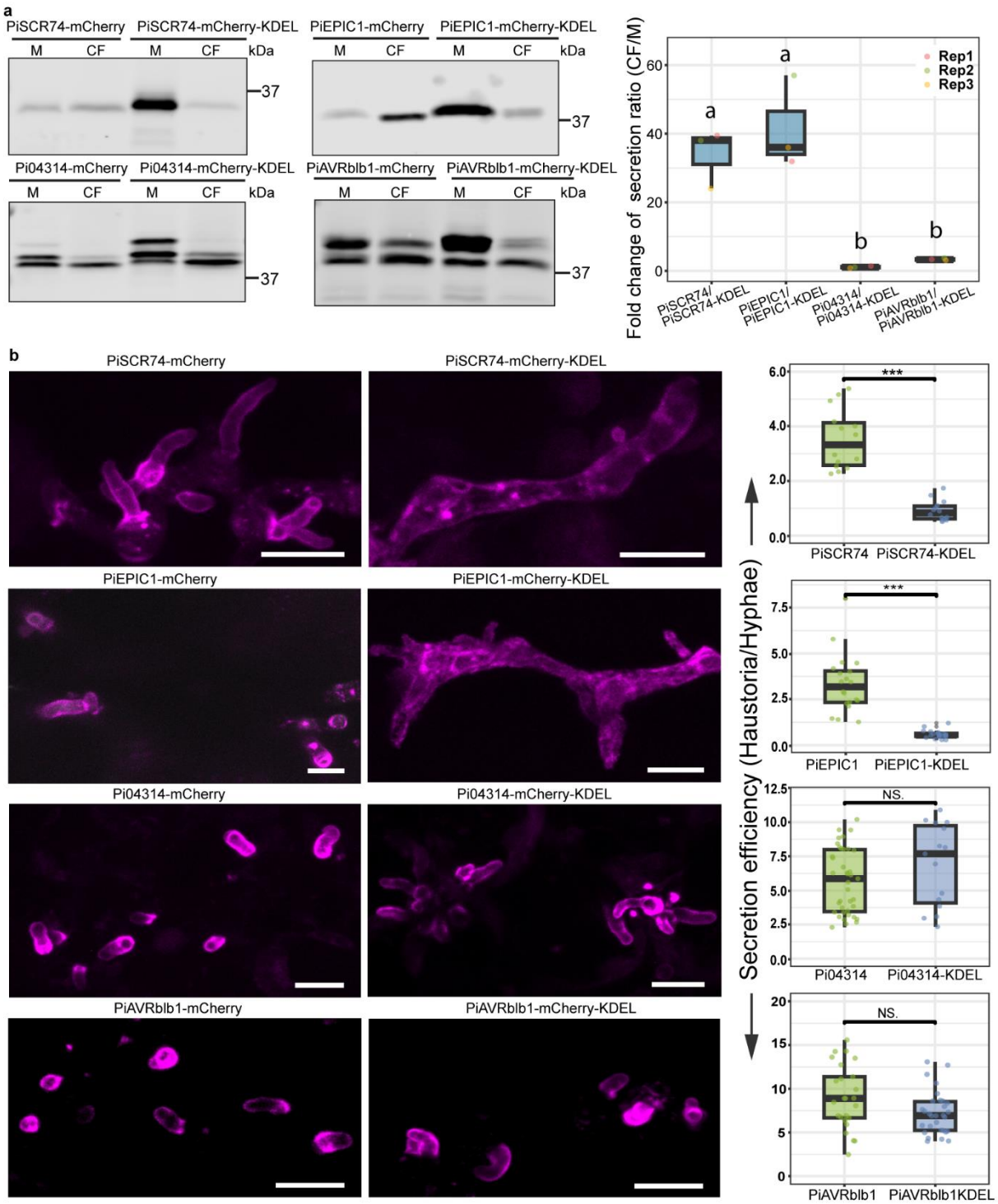

Fig. 2| Apoplastic effectors secreted via Golgi but RXLR effectors take an alternative route.

a, Immunoblot analysis shows retention of apoplastic effector fusions PiSCR74-mCherry and PiEPIC1-mCherry inside mycelia when fused to a KDEL motif, compared to efficient secretion in their unmodified counterparts. In contrast, the secretion efficicy of RXLR effector fusions Pi04314-mCherry and PiAVRblb1-mCherry was not significantly affected by the addition of the KDEL motif. Protein sizes are indicated in kDa. Quantification of the results is presented in the accompanying boxplot, highlighting the significantly greater impact of the KDEL motif on the secretion of apoplastic effectors compared to RXLR effectors. Secretion efficiency was

541 calculated as the ratio of protein intensity in culture filtrate (CF) to that in mycelial extracts
542 (M). Fold changes represent the difference in CF/M ratios between unmodified and KDEL-
543 containing versions. Data are presented as mean ± SD from three biological replicates indicated
544 by small solid circles. Statistical analysis was performed using one-way ANOVA with post-hoc
545 Tukey HSD test to determine significance. **b,** Confocal microscopy images of infectious
546 hyphae in potato leaf tissue showing that the accumulation of PiSCR74-mCherry and PiEPIC1-
547 mCherry at haustoria is markedly reduced when appended with a KDEL motif, compared to
548 their unmodified versions *in planta*. In contrast, accumulation of Pi04314-mCherry and
549 PiAVRblb1-mCherry at haustoria is not significantly affected by the addition of KDEL.
550 Quantification of the results is presented in the accompanying box plots. Secretion efficiency
551 was calculated based on the fluorescence intensity ratio between haustoria and adjacent hyphae
552 area. Data are presented as mean ± SD from three biological replicates. Individual data points
553 are represented by small solid circles. Statistical analysis was performed using student's *t*-test.
554 Scale bars: 10 µm.
555

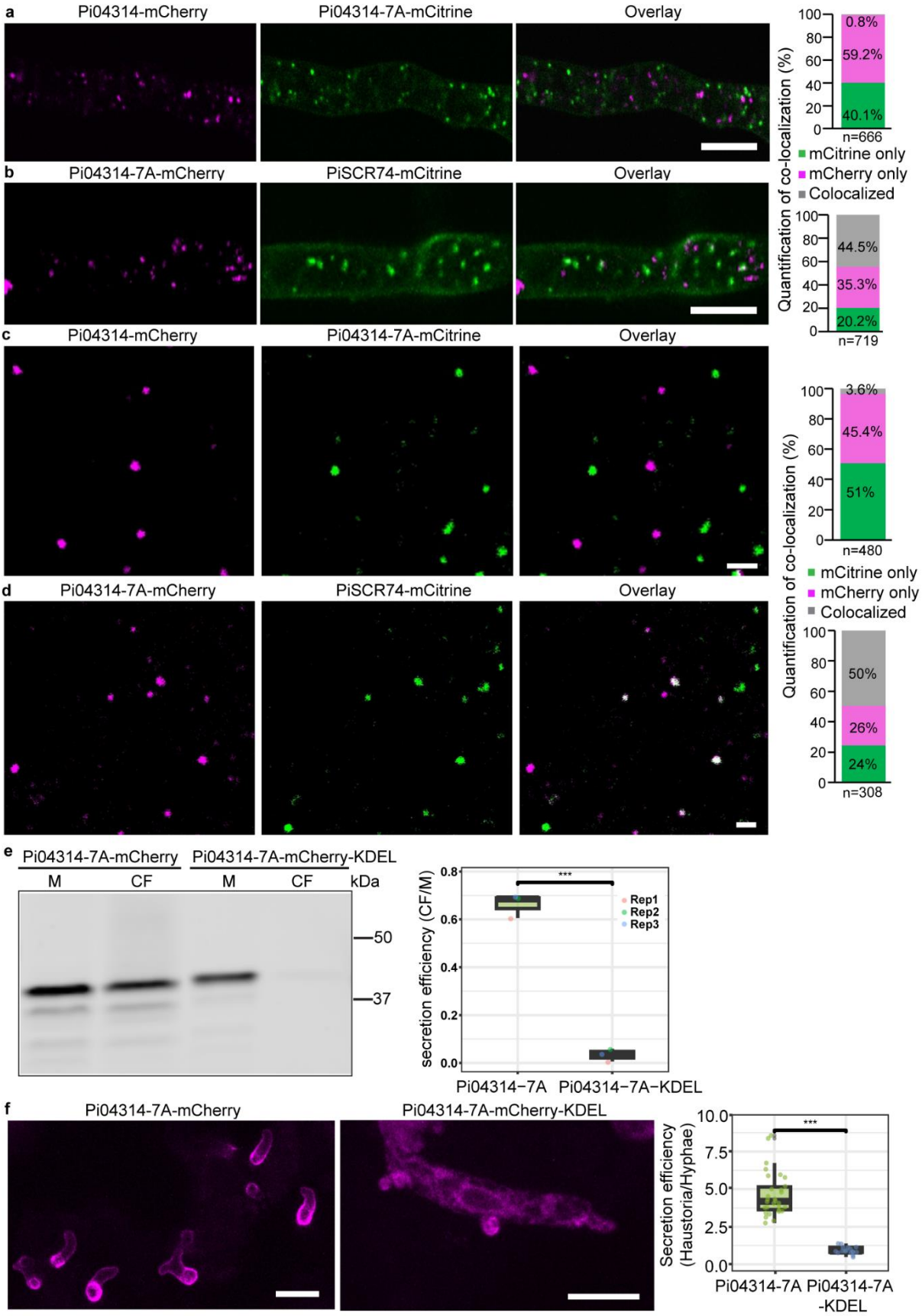
a
Pi04314-mCherry
Pi04314-7A-mCitrine
Overlay
0.8%
59.2%
40.1%
n=666
b
Pi04314-7A-mCherry
PiSCR74-mCitrine
Overlay
44.5%
35.3%
20.2%
n=719
c
Pi04314-mCherry
Pi04314-7A-mCitrine
Overlay
3.6%
45.4%
51%
n=480
d
Pi04314-7A-mCherry
PiSCR74-mCitrine
Overlay
50%
26%
24%
n=308
Quantification of co-localization (%)
mCitrine only
mCherry only
Colocalized
e
Pi04314-7A-mCherry
Pi04314-7A-mCherry-KDEL
M
CF
M
CF
kDa
50
37
secretion efficiency (CF/M)
Rep1
Rep2
Rep3
Pi04314−7A
Pi04314−7A−KDEL
f
Pi04314-7A-mCherry
Pi04314-7A-mCherry-KDEL
Secretion efficiency (Haustoria/Hyphae)
Pi04314-7A
Pi04314-7A -KDEL

556
557
558

559 **Fig. 3| RXLR-EER motifs determine secretion pathways. a**, Confocal microscopy images
560 showing wild-type Pi04314-mCherry does not colocalize with the RXLR mutant effector
561 Pi04314-7A-mCitrine. **b**, In contrast, colocalization of PiSCR74-mCitrine with Pi04314-7A-
562 mCherry was observed in cultured hyphae. Scale bars, 10 µm. **c**, Endosomal vesicles isolated
563 from the same dual transformants as in **a** confirm that Pi04314-7A does not colocalize with
564 wild-type Pi04314. **d**, Confocal microscopy shows colocalization of Pi04314-7A with the
565 apoplastic effector PiSCR74. Quantification of colocalization is shown in the accompanying
566 graphs. The numbers of total (n) and co-labelled puncta were determined using the DiAna
567 plugin in Fiji (**a-d**). Scale bars, 2 µm. **e**, Immunoblot analysis reveals that Pi04314-7A-
568 mCherry-KDEL is largely retained in the mycelia (M) while secretion of the unmodified variant
569 is readily detected in the culture filtrate (CF). Secretion efficiency was determined by
570 calculating the ratio of protein abundance in the culture filtrate (CF) relative to that in M.
571 Quantification of the protein secretion efficiency is presented in the accompanying boxplot.
572 Data are presented as mean ± SD from three biological replicates indicated by small solid
573 circles. Protein sizes are indicated in kDa. **f**, Confocal microscopy images of infectious hyphae
574 in potato leaf tissue show that Pi04314-7A-mCherry secretion at haustoria is significantly
575 diminished when fused to a KDEL motif, compared to the intense haustorial signal observed
576 with the unmodified version *in planta*. Quantitative analysis is shown in the accompanying
577 boxplots, where secretion efficiency was assessed by calculating the fluorescence intensity
578 ratio between haustoria and hyphae. Data are expressed as mean ± SD from three independent
579 biological replicates, with individual measurements represented by solid dots. Statistical
580 significance was determined using student's *t*-test. *** indicates $p<0.001$ (**e**, **f**). Scale bars, 10
581 µm.
582
583
584
585
586
587
588
589
590
591
592
593

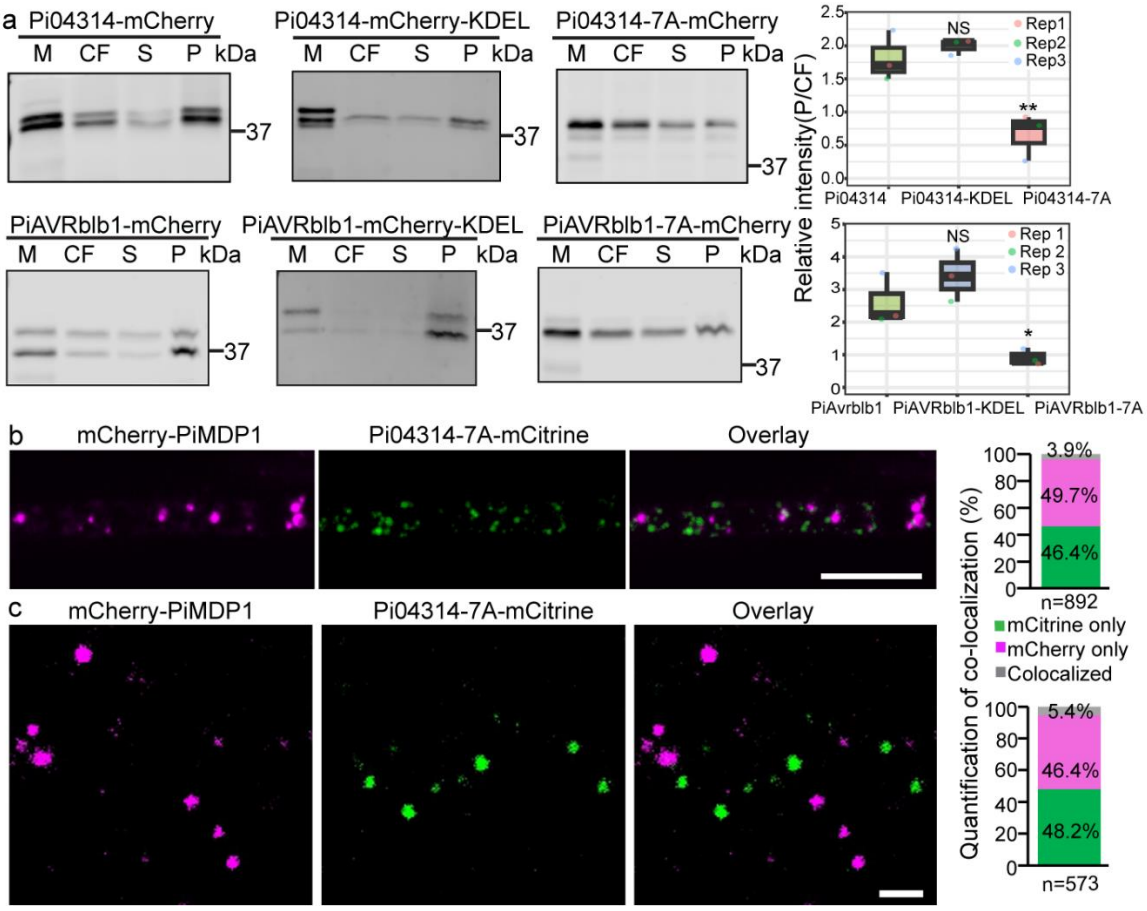

Fig. 4 | RXLR-EER motifs determine the association of effectors with extracellular vesicles (EVs) a, Immunoblot analysis of protein preparations of different fractions from cultured hyphae shows that RXLR effector fusions Pi04314-mCherry, PiAVRblb1-mCherry and their KDEL-modified variants are predominantly enriched in the pellet (P) fraction which contains EVs, whereas the RXLR-EER mutant variant displays markedly reduced association with the pellet fraction. Quantification of protein levels in the pellet fraction relative to that in the culture filtrate (CF) is shown in the accompanying boxplot. Data are expressed as mean ± SD from three independent biological replicates, with individual values represented by solid circles. Statistical analysis was performed using ordinary one-way ANOVA with Dunnett's multiple comparisons test to determine significance. M= mycelia; S=supernatant. Protein sizes are indicated in kDa. **b**, Confocal microscopy images show that mCherry-PiMDP1 and Pi04314-7A-mCitrine do not colocalize in cultured hyphae. Scale bars, 10 µm. **c**, Endosomal vesicles isolated from the same dual transformants as in **b** confirm the absence of colocalization of Pi04314-7A and PiMDP1. Quantitative analysis of colocalization is presented in the accompanying graphs. The percentage of the total numbers of puncta (n) that were colocalized was measured using the DiAna plugin in Fiji (**b**, **c**). Scale bars, 2 µm.